scientific reports

Check for updates

OPEN

MicroRNA-150-3p enhances the antitumour effects of CGP57380 and is associated with a favourable prognosis in non-small cell lung cancer

Hongmei Zheng, Songqing Fan, Jiadi Luo, Qiuyuan Wen & Hongjing Zang✉

MicroRNA (miRNA) dysregulation has been identified in several carcinomas, including non-small cell lung cancer (NSCLC), and is known to play a role in the development and progression of this disease. We initially conducted a miRNA microarray analysis, which revealed that the MNK inhibitor CGP57380 increased the expression of miR-150-3p. A similar analysis was performed using data from The Cancer Genome Atlas (TCGA). Cell proliferation, colony formation and migration assays were validated in A549 and H157 cells treated with miR-150-3p mimics. Quantitative polymerase chain reaction (qPCR) was then used to detect potential target genes. We observed significant downregulation of miR-150-3p in NSCLC samples compared with normal samples ($P = 0.035$). High miR-150-3p expression was associated with longer overall survival ($P = 0.005$), as determined via a tissue microarray (TMA). These results were validated in the TCGA and revealed that miR-150-3p was expressed at low levels in NSCLC tissues ($P < 0.0001$) and that patients with high miR-150-3p expression had a better prognosis ($P = 0.042$). Moreover, the combination of miR-150-3p and CGP57380 exerted a synergistic inhibitory effect on colony formation, growth, and migration and induced apoptosis in NSCLC cell lines. We investigated the potential targets of miR-150-3p and successfully validated six potential target genes through qPCR analysis. High miR-150-3p expression may enhance the response to immunotherapy, cisplatin and gemcitabine. In summary, this study underscores the promising therapeutic implications of combining miR-150-3p and CGP57380 for NSCLC treatment. Additionally, this study provides valuable insights into the molecular mechanisms underlying the effects of this treatment.

Keywords Non-small cell lung cancer, MNK inhibitor, MicroRNA, Targeted therapy

Lung cancer is broadly categorized into two pathological subtypes: non-small cell lung cancer (NSCLC) and small cell lung cancer (SCLC)[1]. NSCLC encompasses various subtypes, including adenocarcinoma, squamous cell carcinoma, and large cell carcinoma, and accounts for the majority (approximately 80–85%) of all lung cancer cases[1]. Among NSCLC subtypes, adenocarcinoma is the most prevalent and is commonly found in the peripheral regions of the lung. Nevertheless, despite advancements in early diagnostic methods and the application of targeted and immunotherapeutic treatments, the prognosis of NSCLC patients remains unfavourable, with a five-year survival rate of approximately 21%[2]. These statistics underscore the great need for ongoing research and for the development of innovative therapeutic strategies to improve outcomes for individuals diagnosed with NSCLC.

Emerging evidence supports the critical involvement of eukaryotic translation initiation factor 4E (eIF4E) and its downstream effectors, mitogen-activated protein kinase-interacting kinases (MNKs), in cancer drug resistance[3,4]. MNKs have been shown to promote drug resistance across various cancer types, including lung, breast, and pancreatic cancers[5–7]. Several studies have established that MNKs can confer resistance to chemotherapy in patients with pancreatic cancer[7] and breast cancer[8]. Our team previously confirmed that the mTOR inhibitor rapamycin induces eIF4E phosphorylation through MNK activation in NSCLC[9]. CGP57380, an MNK inhibitor, effectively abolishes mTOR inhibitor-induced eIF4 phosphorylation and Akt activation[9].

Department of Pathology, The Second Xiangya Hospital of Central South University, Changsha, China. ✉email: zanghongjing@csu.edu.cn

MicroRNAs (miRNAs) are a class of small noncoding RNA molecules that have emerged as promising biomarkers and therapeutic targets in the context of lung cancer[10]. To further understand the specific mechanism of miRNAs, we performed a miRNA microarray analysis to detect changes in miRNAs induced by CGP57380 treatment. Among the differentially expressed genes, miR-150-3p attracted our attention. Recent investigations have elucidated the inhibitory effects of miR-150-3p on cell proliferation in various tumour types, including gliomas, hepatocellular carcinoma, colorectal cancer, and head and neck squamous cell carcinoma (HNSCC)[11–14]. The role of miR-150 in tumours involves various aspects, such as matrix metalloproteinases, cell adhesion, transcription factors, and epigenetics[15–18]. In some studies, miR-150 expression was found to be elevated in lung cancer, whereas in other studies, its expression was decreased[19–21]. These findings emphasize the need for further research to better comprehend the contradictory observations of miR-150 in NSCLC. MiR-150-3p is a passenger strand miRNA of pre-miR-150. We first reported that miR-150-3p may be associated with therapeutic resistance caused by MNKs in non-small cell lung cancer.

In this study, we explored the potential antitumour effects of CGP57380 and miR-150-3p in NSCLC. Our findings revealed that CGP57380 can upregulate the expression of miR-150-3p, as evidenced by miRNA microarray analysis. The combined approach of miR-150-3p overexpression and CGP57380 treatment synergistically inhibited NSCLC cell survival, colony formation, growth, and migration and simultaneously induced apoptosis. Additionally, we provide insights into the downstream targets and regulatory mechanisms of miR-150-3p in NSCLC to reveal its potential antitumour effects. These findings suggest that targeting miR-150-3p and CGP57380 may have significant therapeutic implications for the treatment of NSCLC.

Materials and methods

Reagents

The primary antibodies against Mcl-1 (#94296), cleaved-PARP (#5625), Bcl-2 (#15071) and c-caspase 3 (#9664) (#8592) were purchased from Cell Signaling Technology (Beverly, MA, USA) and were used at a 1:1,000 dilution. E-cadherin used at a 1:2,000 dilution and α-tubulin used at a 1:5,000 dilution were procured from Proteintech (Wuhan, Hubei, P.R.C.). CGP57380 was obtained from Selleckchem (Houston, TX, USA).

Cell lines and cell culture

The human NSCLC cell lines A549 and H157 were acquired from the Cell Bank of the Chinese Academy of Sciences (Shanghai, China). Cells were cultured in RPMI-1640 medium (Gibco, USA) supplemented with 10% foetal calf serum (Gibco, USA) in a humidified incubator at 37 °C with 5% CO_2.

MiRNA microarray analysis

For the miRNA microarray analysis, cells were seeded in cell culture plates at a density of 1×10^5 cells per well in triplicate. The following day, they were treated with either vehicle or 25 μM CGP57380. After 24 h of treatment, total RNA was extracted using TRIzol reagent (Invitrogen), and the miRNA microarray analysis was performed as previously described[22].

Quantitative RT–PCR analysis

Total RNA preparation and RT-PCR analysis were conducted as previously described[22]. The forward primer used was 5′-CTGGTACAGGCCTGGGGGACAG-3′ (miR-150-3p), along with a universal primer against the stem-loop region 5′-GTGCAGGGTCCGAGGT-3′.

Western blot analysis

The procedures for the preparation of whole-cell protein lysates and western blot analysis followed established protocols[22]. To conserve time and antibody resources, and considering that the antibodies are frequently utilized in our laboratory, we have chosen to cut the Western blot membrane.

Colony formation and transwell migration assays

Colony formation assays were performed in 6-well plates, whereas Transwell migration assays were performed in 24-well plates containing inserts (Costar 3422; Corning Inc., Corning, NY, USA). Protocols for both colony formation and Transwell migration assays were conducted according to previously established methods[22].

MiRNA mimic preparation and transfection

The synthetic miR-150-3p mimics and NC mimics (GenePharma, Shanghai, China) were resuspended in DEPC water at a concentration of 20 μM. The transfection protocols for the miRNA mimics were performed as previously described by our team[22].

Cell proliferation and apoptosis assays

Cells were seeded in 96-well plates and treated with the experimental agents on the second day. After a specified treatment period, cell viability was assessed via a CCK8 assay according to previously described procedures[22]. To evaluate cell apoptosis, an Annexin V/FITC apoptosis detection kit (Beyotime Biotechnology, China) was used in accordance with the manufacturer's instructions.

In situ hybridization and scores

The optimal staining conditions for the miR-150-3p probe were determined according to our laboratory's prior experience. We utilized TMA technology to design and construct high-throughput NSCLC TMAs that adhered to previously described guidelines. In situ hybridization (ISH) and scoring were conducted via well-established methods reported in our previous publications[22]. The evaluation method was as follows: the staining intensity of

miR-150-3p was scored as 3 (strong), 2 (moderate), 1 (weak), or 0 (negative), while the staining percentage was scored as 4 (76-100%), 3 (51-75%), 2 (26-50%), 1 (1-25%), or 0 (0%). The total scores for miR-150-3p ranged from 0 to 12, with an optimal cut-off level of 2 determined by the log-rank test. Finally, we classified miR-150-3p expression into high expression and low expression categories.

Biological information analysis

To gain insight into the molecular mechanisms underlying our findings, we conducted Gene Ontology (GO) enrichment analysis and Kyoto Encyclopedia of Genes and Genomes (KEGG) pathway analysis. These analyses were performed using the DAVID online tool (https://david.ncifcrf.gov/). We sought to not only understand the molecular pathways involved, but we also assessed tumour immune infiltration using the ESTIMATE[23] and XCELL[24] algorithms in R software. To evaluate the potential immunotherapy response, we utilized the Tumor Immune Dysfunction and Exclusion (TIDE)[25] score as a biomarker. To predict the chemotherapy and targeted therapy drug responses for each sample, we employed the oncoPredict R package[26]. This comprehensive approach allowed us to better understand the biological and immunological context surrounding our research findings.

Statistical analysis

All statistical analyses were performed using SPSS version 19 (SPSS, Chicago, IL). The relationships between miR-150-3p expression and the clinicopathological features of patients with NSCLC were assessed using a chi-square test. Kaplan–Meier analysis was performed to generate overall survival (OS) curves, and the log-rank test was used to determine statistical significance. A Cox proportional hazard regression model was used to assess whether miR-150-3p serves as an independent prognostic factor. Other statistically significant differences were determined via one-way analysis of variance (ANOVA). Two-sided statistical analyses were conducted, and a significance level of $P < 0.05$ indicated statistical significance.

Results

The Mnk inhibitor CGP57380 increases mir-150-3p expression in NSCLC

To gain a comprehensive understanding of the impact of the Mnk inhibitor CGP57380 on global microRNA expression, we performed experiments using the Agilent Human miRNA chip V21.0 (Agilent Technologies Inc.). Our analysis revealed that 55 miRNAs were upregulated, whereas 55 miRNAs were downregulated (fold change > 2.0 and $P < 0.05$) (Fig. 1A&B). Notably, among the miRNAs upregulated by CGP57380, miR-150-3p attracted our attention. Although the role of miR-150 has been confirmed in various tumours, its specific role in lung cancer remains to be further elucidated. Previous studies have focused mostly on miR-150-5p, but our miRNA chip results indicated that the expression of the passenger miRNA miR-150-3p was significantly increased by CGP57380 (FC > 2.0 and $P < 0.05$) (Fig. 1A&B). RT-PCR analysis confirmed that CGP57380 could stimulate the expression of miR-150-3p in a concentration-dependent manner (Fig. 1C). Using data from the TCGA database, we confirmed that miR-150-3p was downregulated in NSCLC tissues compared with normal tissues (Fig. 1D). Importantly, our results demonstrated that NSCLC patients with high miR-150-3p expression levels experienced significantly longer overall survival than those with low levels ($P = 0.042$) (Fig. 1E). This intriguing discovery prompted additional investigation into the potential significance of miR-150-3p and further validation in NSCLC.

Associations between Mir-150-3p expression and the clinical features of NSCLC patients

To identify the role of miR-150-3p in NSCLC, our team constructed tissue microarrays (TMAs) consisting of NSCLC samples and noncancerous normal lung tissue[27]. The methods for constructing and scoring these TMAs containing both NSCLC and corresponding normal lung tissues are described in our previous publications[27,28]. We evaluated the expression and subcellular location of miR-150-3p in 90 noncancerous normal lung tissues and 272 NSCLC tissues using in situ hybridization (ISH). Standard evaluations of different paraffin-embedded tissues are shown in Fig. 2A. MiR-150-3p was expressed primarily in the cytoplasm (Fig. 2A). The positive expression rate of miR-150-3p in NSCLC tissues was lower than that in normal tissues ($P = 0.035$) (Fig. 2B).

We then examined the relationships between miR-150-3p expression and the clinical features of NSCLC patients, including overall survival (OS), lymph node metastasis, and tumour stage (Tables 1 and 2). The expression of miR-150-3p was significantly associated with prolonged overall survival (OS) ($P = 0.005$) (Fig. 2C). MiR-150-3p expression was also more prevalent in NSCLC patients without lymph node metastasis ($P = 0.013$) (Table 1). Additionally, our study revealed that patients with a lower pathological stage had a longer OS ($P = 0.021$) (Table 2) and that those with earlier clinical disease (stage I) exhibited superior OS compared with those with advanced disease (stages II and III) ($P = 0.004$) (Table 2). Patients without lymph node metastasis also exhibited longer OS ($P = 0.014$) (Table 2). Interestingly, using bioinformatics analysis, we discovered that high miR-150-3p expression was associated with improved OS in patients with cervical squamous cell carcinoma and endocervical adenocarcinoma (CESC), skin cutaneous melanoma (SKCM), and uterine corpus endometrial carcinoma (UCEC) ($P = 0.004274$, $P = 0.01648$, $P = 0.0128$) (Supplementary Fig. 1A-C). These findings reinforce the robustness of our TMA data and emphasize the potential of miR-150-3p as a valuable independent prognostic indicator. Our ongoing research aims to elucidate how miR-150-3p impacts NSCLC and to explore new avenues for the treatment of this disease.

Effects of ectopic expression of mir-150-3p and CGP57380 in an NSCLC cell line

Initially, we found that miR-150-3p was underexpressed in NSCLC cell lines, including A549, H157 and SPC-A1, compared with the nontumorigenic human bronchial epithelial (HBE) cell line (Supplementary Fig. 1D). We then focused on the H157 and A549 cell lines. The transfection efficiency of the miR-150-3p mimics in the H157 and A549 cell lines is displayed in Supplementary Fig. 1E.

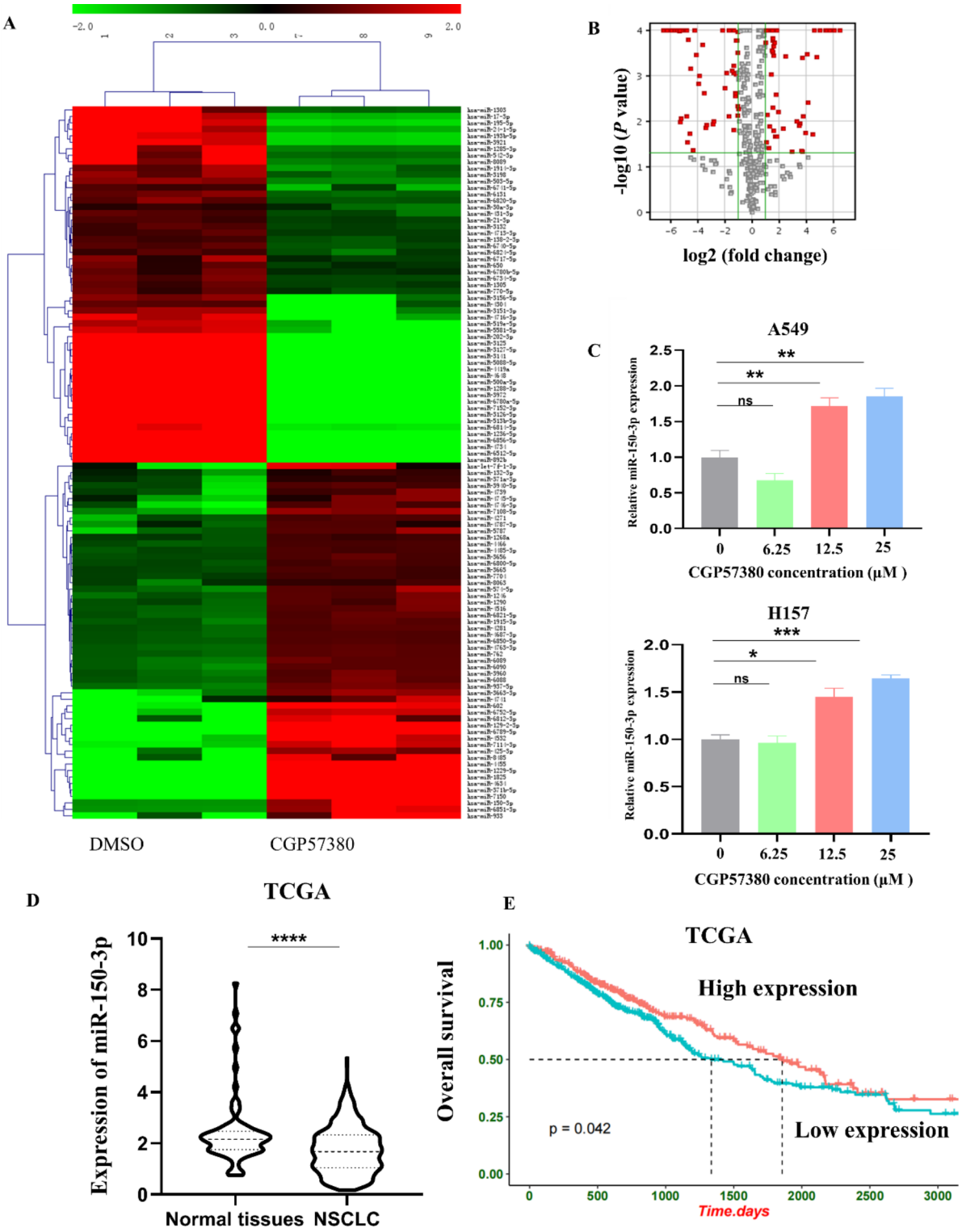

Fig. 1. Cluster heatmap of miRNA profiles in the CGP57380 and control treatment groups based on the results of the miRNA microarray analysis (FC > 2.0 and $P < 0.05$). **A** & **B**. Cluster heatmap of miRNA expression differences between the CGP57380 and control treatment groups. **C**. The expression of miR-150-3p was measured by qRT-PCR in A549 and H157 cells treated with different concentrations of CGP57380. **D**. Differential expression of miR-150-3p was observed in NSCLC and noncancerous tissues in the TCGA database. **E**. High expression of miR-150-3p was associated with better overall survival of NSCLC patients in the TCGA database ($P = 0.042$). ($*P < 0.05$, $**P < 0.01$, and $***P < 0.001$).

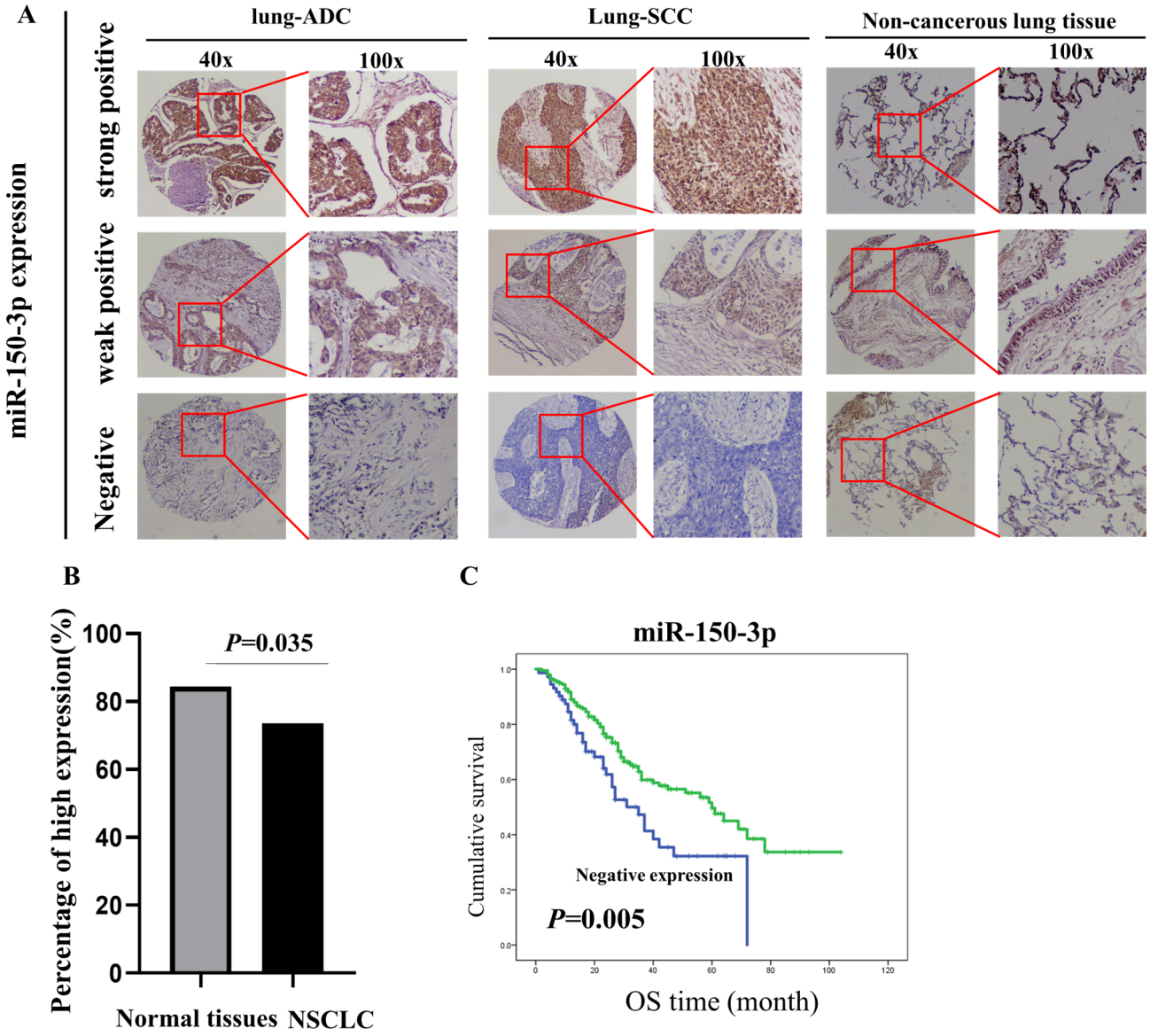

Fig. 2. MiR-150-3p expression in NSCLC. **A**. Representative in situ hybridization (ISH) staining of miR-150-3p in lung adenocarcinoma (ADC, squamous cell carcinoma (SCC), and noncancerous lung tissue using a specific probe. DAB staining shows that positive expression of miR-150-3p was predominantly localized in the cytoplasm. The magnification was 40 × and 100 ×. **B**. MiR-150-3p expression in NSCLC and normal tissues was measured via qRT-PCR. C. The expression of miR-150-3p was significantly associated with longer overall survival (OS) ($P = 0.005$).

Compared with that of control cells, the proliferation of A549 and H157 cells was inhibited by transfection with miR-150-3p (Fig. 3A). Colony formation and migration activities were also significantly suppressed after transfection with miR-150-3p (Fig. 3B-C).

The synergistic effects of the ectopic expression of miR-150-3p and CGP57380 were investigated using proliferation and migration assays after combination treatment of A549 and H157 cell lines with miR-150-3p and CGP57380. Compared with individual treatment, combined treatment consisting of ectopic miR-150-3p expression and CGP57380 resulted in greater reductions in cancer cell proliferation and colony formation (Fig. 3A-C). Apparent synergistic effects were also observed following both ectopic miR-150-3p expression and CGP57380 treatment. Therefore, we next discuss the possible mechanisms of the combination treatment.

Cotreatment with mir-150-3p and CGP57380 induces apoptosis in NSCLC

We next assessed whether the combination of a miR-150-3p mimic and CGP57380 effectively decreased the survival of NSCLC cell lines by inducing apoptosis. As evaluated by Annexin V/PI flow cytometry, the combination of miR-150-3p and CGP57380 significantly induced cell apoptosis compared with each agent alone (Fig. 4A-B). Western blot assays confirmed these results. The protein expression levels of cleaved-PARP, cleaved-

Variables	miR-150-3p expression		
	Negative (%)	Positive (%)	*p*
Age (years)			
<60 (*n* = 175)	51 (29.1%)	124 (70.9%)	0.180
≥60 (*n* = 97)	21 (21.6%)	76 (78.4%)	
Gender			
Female (*n* = 69)	15 (21.7%)	54 (78.3%)	0.302
Male (*n* = 203)	57 (28.1%)	146 (71.9%)	
Histological type			
LUAD (*n* = 139)	34 (24.5%)	105 (75.5%)	0.442
LUSC (*n* = 133)	38 (28.6%)	95 (71.4%)	
Pathological grade			
Well/moderate (*n* = 128)	38 (29.7%)	90 (70.3%)	0.257
Poor (*n* = 144)	34 (23.6%)	110 (76.4%)	
Clinical stage			
Stage I (*n* = 131)	32 (24.4%)	99 (75.6%)	0.462
Stage II and III (*n* = 141)	40 (28.4%)	101 (71.6%)	
LNM status			
LNM (*n* = 155)	50 (32.3%)	105 (67.7%)	0.013 *
No LNM (*n* = 117)	22 (18.8%)	95 (81.2%)	

Table 1. Associations between Mir-150-3p expression and clinicopathological features in patients with NSCLC (*n* = 272). Abbreviations: LUAD: lung adenocarcinoma; LNM: lymph node metastasis; LUSC: lung squamous cell carcinoma; *: $p < 0.05$.

Parameters	Univariate analysis			Multivariate analysis		
	Average survival time (SE)	95% CI	*P*	Exp (B)	95.0% CI	*P*
miR-150-3p						
Negative expression	38.603 (3.609)	(31.529, 45.676)	0.005*	1.593	(1.055, 2.404)	0.027*
Positive expression	59.946 (3.645)	(52.802, 67.090)				
Clinical stage						
Stage I	72.261 (4.657)	(63.133, 81.389)	0.000*	0.525	(0.339, 0.813)	0.004*
Stage II and III	40.948 (2.910)	(35.244, 46.651)				
LNM status						
LNM	42.424 (2.670)	(37.192, 47.657)	0.000*	1.729	(1.118, 2.674)	0.014*
No LNM	67.865 (4.658)	(58.734, 76.996)				
Pathological grade						
Well and moderate	59.518 (3.826)	(52.020, 67.016)	0.002*	0.630	(0.425, 0.932)	0.021*
Poor	49.706 (4.082)	(41.706, 57.707)				
Histological type						
LUAD	50.408 (3.347)	(43.848, 56.968)	0.827	1.306	(0.871, 1.959)	0.196
LUSC	60.406 (4.674)	(51.245, 69.567)				
Gender						
Female	58.966 (4.787)	(49.583, 68.349)	0.105	0.696	(0.431, 1.123)	0.137
Male	52.870 (3.725)	(45.569, 60.171)				
Age						
< 60	58.219 (3.998)	(50.383, 66.055)	0.077	0.763	(0.520, 1.119)	0.167
≥ 60	47.613 (4.287)	(39.211, 56.015)				

Table 2. Univariate and multivariate analyses for OS in NSCLC patients. Abbreviations: OS: overall survival; CI: confidence interval; SE: standard error; Exp(β): odds ratio; LUAD: lung adenocarcinoma; LNM: lymph node metastasis; LUSC: lung squamous cell carcinoma; *: $p < 0.05$.

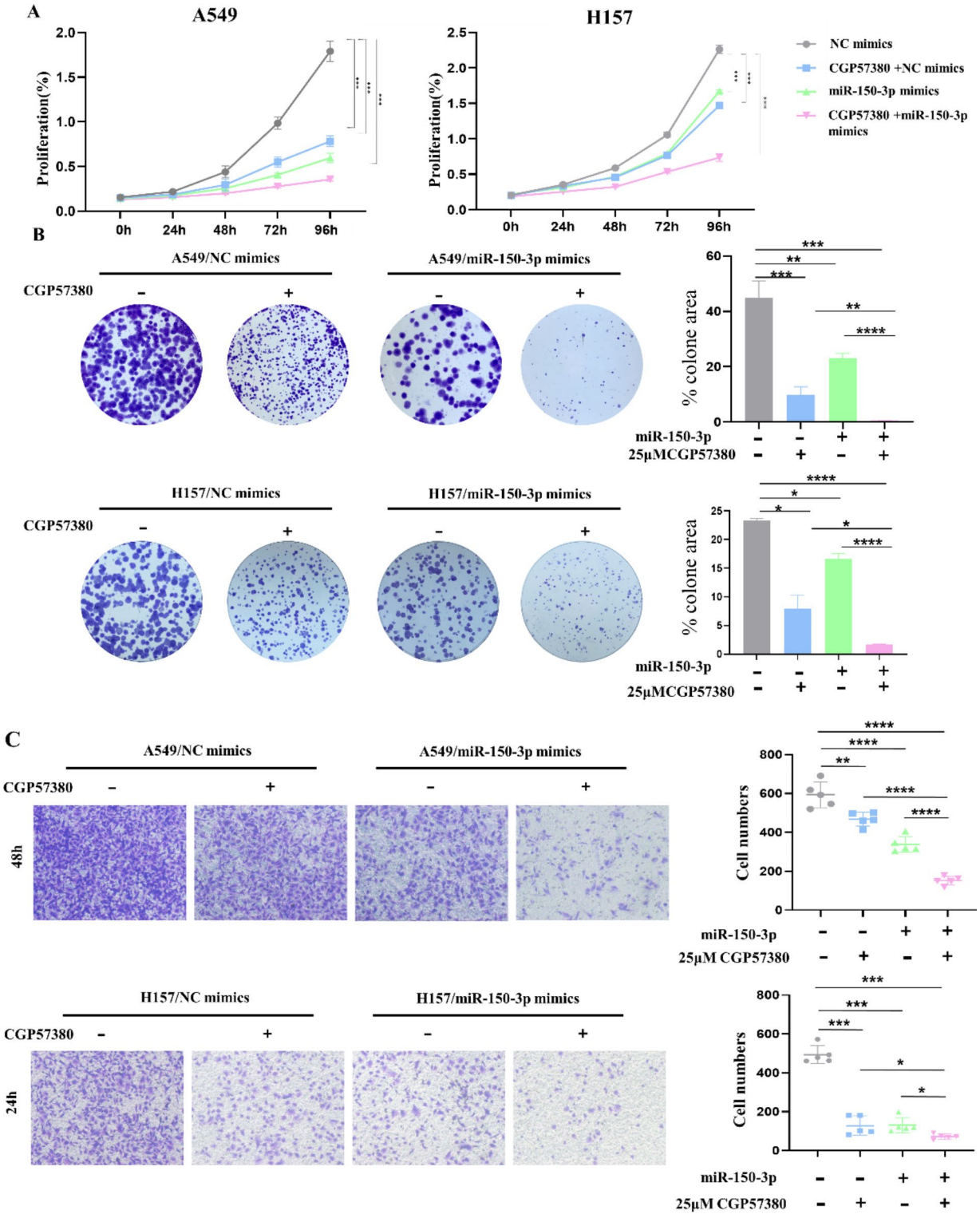

Fig. 3. MiR-150-3p regulates cell proliferation, colony formation and migration of NSCLC cells. **A**. Cell proliferation was evaluated by CCK-8 assay in A549 and H157 cells treated with miR-150-3p mimics, CGP57380, or both. **B**. Colony formation assays were performed to evaluate the effects of miR-150-3p mimics, CGP57380, or both on A549 and H157 cells. **C**. Transwell migration assays were performed to evaluate the effects of miR-150-3p mimics, CGP57380, or both on A549 and H157 cell migration. (*$P<0.05$, ** $P<0.01$, and *** $P<0.001$).

Caspase-3 and Bcl-2 were significantly decreased by the combination treatment (Fig. 4C). The reduction in Bcl-2 expression, along with the simultaneous increase in Mcl-1 expression, indicated a compensatory mechanism aimed at counterbalancing the deficiency in antiapoptotic signalling caused by Bcl-2 downregulation. Furthermore, we observed increased protein expression of E-cadherin (Fig. 4C), which provides additional evidence of antitumour effects in the combination treatment group. Collectively, these findings underscore the potential of combining miR-150-3p overexpression with CGP57380 as a promising strategy to induce apoptosis in NSCLC cells. This therapeutic approach has significant implications for future investigations and holds promise for the development of novel treatment modalities for NSCLC patients.

Identification of putative target genes regulated by miR-150-3p

To delve deeper into the mechanisms underlying our findings, we used three databases (miRDB, TargetScan, and miRWalk) to predict potential downstream target genes of miR-150-3p. This analysis revealed 347 common target genes (Fig. 5), which were subsequently subjected to KEGG and GO (biological process, molecular function, and cellular component) enrichment analyses using the DAVID online tool to identify potential pathways and biological functions that may be involved (Fig. 5B-C). Our results revealed that the predicted target genes were enriched in pathways associated with cancer, AMPK signalling, ErbB signalling, PI3K-Akt signalling, and several other pathways (Fig. 5C). Additionally, GO enrichment analysis was conducted, the results of which are summarized in Fig. 5B. Through a combination of literature review and qPCR validation, we identified six potential target genes (DAZAP2, FBXL5, PTGFRN, RUNX1, ACACA and ADAM12) from the pool of 347 common genes (Fig. 5D). These findings provide valuable insights into the potential mechanisms that underlie the differences in immune cell composition and treatment response observed in NSCLC patients with high miR-

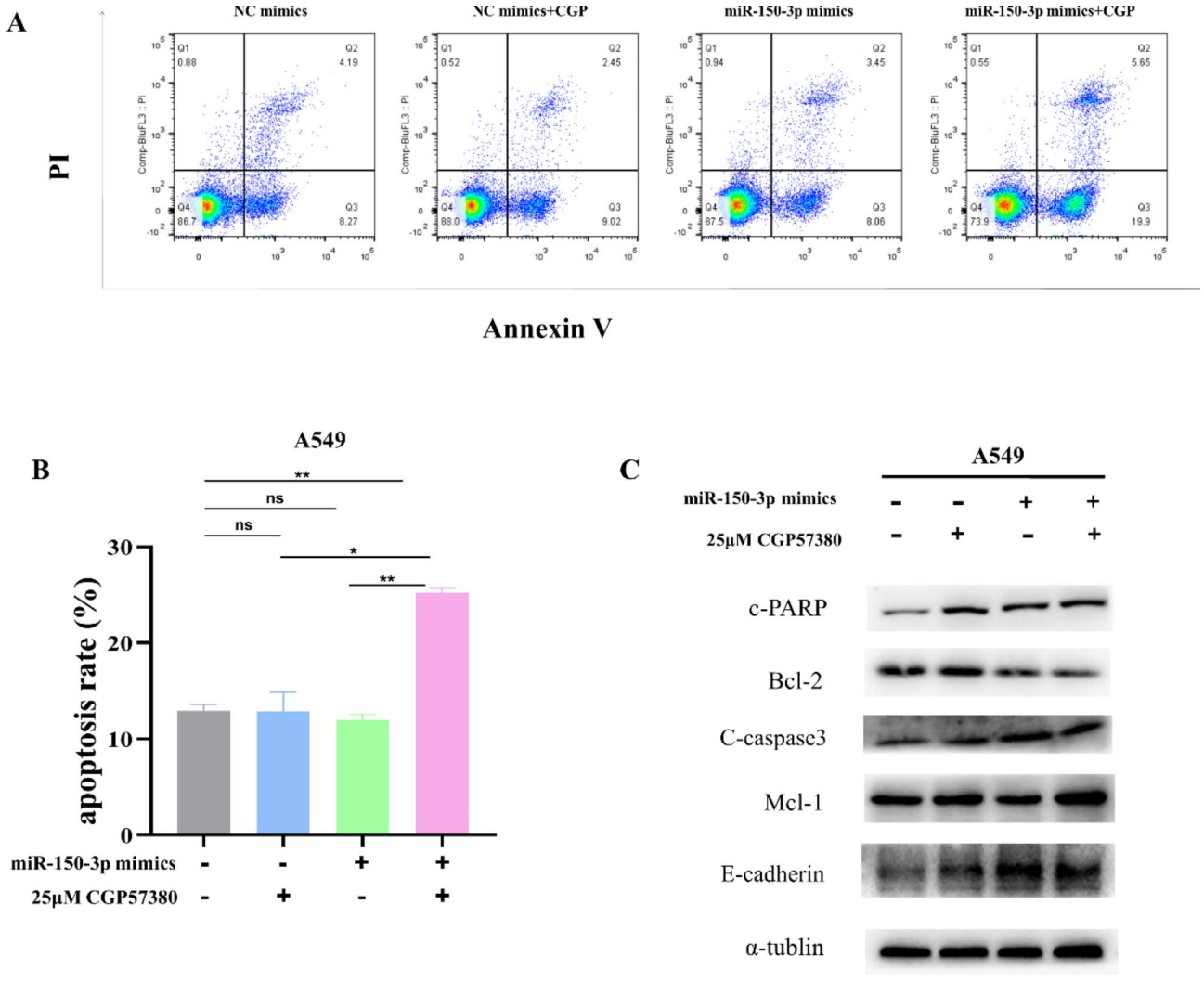

Fig. 4. Combination treatment consisting of miR-150-3p and CGP57380 regulates cell apoptosis in NSCLC cells. **A** & **B**. Apoptosis was detected via Annexin V/flow cytometry in A549 cells treated with miR-150-3p mimics, CGP57380, or both. **C**. Western blot analysis of protein expression levels in A549 cells treated with miR-150-3p mimics, CGP57380, or both (* $P<0.05$, ** $P<0.01$, and *** $P<0.001$).

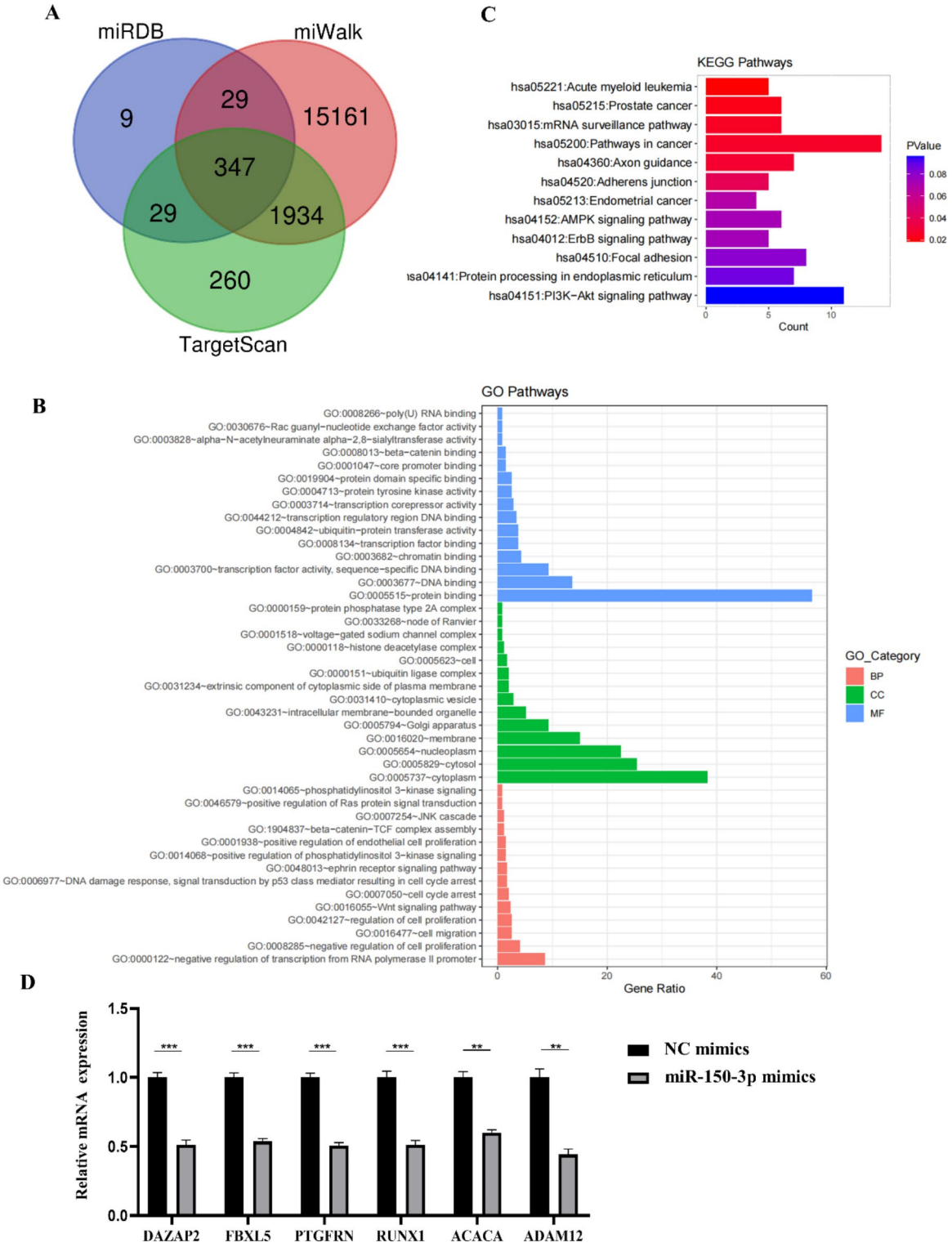

Fig. 5. Identification and functional analysis of miR-150-3p target genes. **A**. Venn diagram depicting the overlap of the miRDB, miRWalk, and TargetScan databases, resulting in a total of 347 consensus genes. **B** & **C**. Gene Ontology (GO) and Kyoto Encyclopedia of Genes and Genomes (KEGG) pathway enrichment analyses of the consensus genes were performed using the DAVID online tool. **D**. qPCR analysis of six putative target genes (DAZAP2, FBXL5, PTGFRN, RUNX1, ACACA, and ADAM12) in NSCLC cells treated with miR-150-3p mimics. The mRNA expression levels of all six genes were significantly lower ($P<0.01$ or $P<0.001$) in treated cells than in control cells (** $P<0.01$ and *** $P<0.001$).

150-3p expression. Future studies may involve further exploration of the roles of these target genes and pathways in NSCLC, which could lead to the development of innovative therapeutic strategies.

The relationship between mir-150-3p and the immune microenvironment and its ability to predict treatment efficacy

In our study, we observed 11 different immune cell types within the tumour immune microenvironment as well as a significant disparity in the composition of these cells between the NSCLC patient group with high miR-150-3p expression and the group with low miR-150-3p expression (Supplementary Fig. 2A). Specifically, the expression of B-cell, CD4 + T-cell, naive CD4 + T-cell, class-switched memory B-cell, dendritic cell (DC), multipotent progenitor (MPP), macrophage, preadipocyte, activated dendritic cell (aDC), and plasmacytoid dendritic cell (pDC) markers was elevated in the group with high miR-150-3p expression. Furthermore, we established a significant positive correlation between miR-150-3p expression and the immune score (Supplementary Fig. 2B). These findings suggest that NSCLC patients with high expression of miR-150-3p may be more responsive to immunotherapy, as evidenced by their lower TIDE scores (Supplementary Fig. 2C). Additionally, we observed that NSCLC patients with high miR-150-3p expression exhibited favourable responses to cisplatin and gemcitabine, whereas no significant difference was noted in the response to osimertinib (Supplementary Fig. 2D). These results offer valuable insights into the development of immunotherapeutic strategies for NSCLC patients.

Discussion and conclusion

Our study aimed to elucidate the role of miR-150-3p in NSCLC. MicroRNAs have been well defined as critical regulators of tumour development and progression in NSCLC. Mir-150-3p has previously been characterized as a potent tumour suppressor in breast cancer, colorectal cancer and hepatocellular carcinoma[12–14]. Furthermore, this miRNA can regulate the production and functionality of a diverse array of immune cell types, including T cells, B cells, natural killer cells, and dendritic cells, in liver hepatocellular carcinoma[29]. In our study, we revealed that ectopic expression of miR-150-3p inhibited NSCLC cell proliferation, colony formation and migration. Moreover, combination treatment consisting of CGP57380 and miR-150-3p exerted synergistic antitumour effects through the induction of cell apoptosis.

Initially, using a miRNA microarray, we demonstrated that the Mnk inhibitor CGP57380 can increase the expression of several miRNAs, including miR-150-3p. We subsequently performed RT-PCR to confirm that miR-150-3p expression was increased by CGP57380 and compared a panel of NSCLC cell lines and the normal lung epithelial cell line HBE with respect to decreased mRNA levels of miR-150-3p. In 90 noncancerous normal lung tissues and 272 NSCLC tissues, positive miR-150-3p expression by ISH was associated with better OS and served as an independent prognostic predictor. The results of the TCGA data analysis were similar. Furthermore, the pancancer analysis conducted in this study indicated that miR-150-3p may serve as a superior prognostic predictor in CESC, SKCM and UCEC. These compelling findings underscore the potential of miR-150-3p as a robust prognostic biomarker for NSCLC and emphasize its clinical significance.

Importantly, combination treatment involving the ectopic expression of miR-150-3p and CGP57380 resulted in significant synergistic effects on the inhibition of cell proliferation, colony formation and migration of NSCLC cells. This combination treatment was demonstrated to induce apoptosis of NSCLC cells, which may be the mechanism by which this treatment exerts its antitumour effects. These results emphasize the potential of targeting the Mnk pathway as a viable therapeutic strategy to restore miR-150-3p levels and enhance its antitumour effects in NSCLC.

To elucidate the molecular mechanisms underlying these phenotypic changes, we conducted a comprehensive analysis of potential miR-150-3p target genes. Through the integration of multiple prediction algorithms and experimental validation, we successfully identified six putative target genes that were significantly downregulated upon miR-150-3p overexpression: DAZAP2, FBXL5, PTGFRN, RUNX1, ACACA and ADAM12. Each of these genes has been implicated in various aspects of cancer biology. DAZAP2 is associated with multiple myeloma (MM) carcinogenesis[30]. FBXL5 has been shown to participate in the progression of several cancer types, including pancreatic ductal adenocarcinoma, colon adenocarcinoma, and lung cancer[31–33], which emphasizes its impact on tumorigenesis. Prostaglandin F2 receptor inhibitor (PTGFRN) has demonstrated oncogenic properties in glioblastoma[34]. RUNX1 has been linked to somatic mutations in solid tumours, including breast, oesophageal, endometrial, and ovarian cancers, which highlights its diverse roles in cancer[35]. Acetyl-CoA carboxylase alpha (ACACA) has been associated with hepatocellular carcinoma (HCC) and colorectal tumours[36,37]. ADAM12 has been identified as a potential prognostic factor in rectal cancer patients following radiotherapy[38]. These target genes play crucial roles in the regulation of tumour cell cycle progression, apoptosis, and invasion, as they collectively influence the malignant behaviour of cancer cells. Notably, functional enrichment analysis revealed that the PI3K-AKT and AMPK pathways were enriched in the downregulated genes. These pathways are intimately linked to cancer progression and metastasis, which provides further evidence of the tumour-suppressive role of miR-150-3p in NSCLC. This multifaceted insight into the molecular mechanisms underlying the effects of miR-150-3p contributes to our understanding of its potential as a therapeutic target in NSCLC. Furthermore, we investigated immune cell infiltration and predicted differences in drug response between the high- and low-miR-150-3p expression groups in the TCGA-NSCLC cohort. The immune infiltration, immune score and drug response of the two groups were significantly different. These findings suggest that NSCLC patients with high expression of miR-150-3p may be more responsive to immunotherapy, cisplatin and gemcitabine, while no significant difference was noted in the response to osimertinib.

In summary, our study of miR-150-3p in NSCLC has revealed its substantial potential as both a therapeutic target and a predictive biomarker. Through a series of experimental investigations, we demonstrated that the restoration of miR-150-3p expression, combined with CGP57380, exerts a remarkable antitumour effect on NSCLC cell proliferation, colony formation and migration by inducing apoptosis. Our exploration of target

genes and pathways regulated by miR-150-3p has provided insights into its tumour-suppressive mechanisms. Moreover, our clinical analysis firmly established the clinical relevance of miR-150-3p, as low expression levels were shown to be associated with advanced tumour stage, lymph node metastasis, and poor overall survival in NSCLC patients. Additionally, we altered miR-150-3p expression and assessed its effects on the tumour microenvironment and treatment response.

In conclusion, this study lays the groundwork for future research endeavours aimed at harnessing the therapeutic potential of miR-150-3p-based strategies combined with CGP57380.

Data availability

The datasets used and/or analysed during the current study available from the corresponding author on reasonable request.

Received: 22 June 2024; Accepted: 6 January 2025
Published online: 15 January 2025

References

1. Yang, C. Y., Yang, J. C. & Yang, P. C. Precision Management of Advanced Non-small Cell Lung Cancer. *Annu. Rev. Med.* **71**, 117–136. https://doi.org/10.1146/annurev-med-051718-013524 (2020).
2. Yang, C. Y. et al. Stage Shift improves Lung Cancer Survival: real-world evidence. *J. Thorac. Oncol.* **18**, 47–56. https://doi.org/10.1016/j.jtho.2022.09.005 (2023).
3. Cárdenas, E. L. et al. Design of cell-permeable inhibitors of eukaryotic translation initiation factor 4E (eIF4E) for inhibiting aberrant Cap-Dependent translation in Cancer. *J. Med. Chem.* **66**, 10734–10745. https://doi.org/10.1021/acs.jmedchem.3c00917 (2023).
4. Cárdenas, E. L. et al. Design of Cell-Permeable Inhibitors of Eukaryotic Translation Initiation Factor 4E (eIF4E) for Inhibiting Aberrant Cap-Dependent Translation in Cancer. *bioRxiv* (2023). https://doi.org/10.1101/2023.05.23.541912
5. Zhang, Q., Li, H., Li, Q., Hu, Q. & Liu, B. MNK/eIF4E inhibition overcomes anlotinib resistance in non-small cell lung cancer. *Fundam Clin. Pharmacol.* **37**, 245–252. https://doi.org/10.1111/fcp.12850 (2023).
6. Geter, P. A. et al. Hyperactive mTOR and MNK1 phosphorylation of eIF4E confer tamoxifen resistance and estrogen independence through selective mRNA translation reprogramming. *Genes Dev.* **31**, 2235–2249. https://doi.org/10.1101/gad.305631.117 (2017).
7. Adesso, L. et al. Gemcitabine triggers a pro-survival response in pancreatic cancer cells through activation of the MNK2/eIF4E pathway. *Oncogene* **32**, 2848–2857. https://doi.org/10.1038/onc.2012.306 (2013).
8. Li, Z. et al. Inhibiting the MNK-eIF4E-β-catenin axis increases the responsiveness of aggressive breast cancer cells to chemotherapy. *Oncotarget* **8**, 2906–2915. https://doi.org/10.18632/oncotarget.13772 (2017).
9. Wen, Q. et al. CGP57380 enhances efficacy of RAD001 in non-small cell lung cancer through abrogating mTOR inhibition-induced phosphorylation of eIF4E and activating mitochondrial apoptotic pathway. *Oncotarget* **7**, 27787–27801. https://doi.org/10.18632/oncotarget.8497 (2016).
10. Liao, Y. et al. Non-coding RNAs in lung cancer: emerging regulators of angiogenesis. *J. Transl Med.* **20**, 349. https://doi.org/10.1186/s12967-022-03553-x (2022).
11. Tan, Z., Jia, J. & Jiang, Y. MiR-150-3p targets SP1 and suppresses the growth of glioma cells. *Biosci. Rep.* **38** https://doi.org/10.1042/bsr20180019 (2018).
12. Yugawa, K. et al. Cancer-associated fibroblasts promote hepatocellular carcinoma progression through downregulation of exosomal miR-150-3p. *Eur. J. Surg. Oncol.* **47**, 384–393. https://doi.org/10.1016/j.ejso.2020.08.002 (2021).
13. Li, S. et al. Ginsenoside Rh2 suppresses colon cancer growth by targeting the miR-150-3p/SRCIN1/Wnt axis. *Acta Biochim. Biophys. Sin (Shanghai)*. **55**, 633–648. https://doi.org/10.3724/abbs.2023032 (2023).
14. Koshizuka, K. et al. Antitumor Mir-150-5p and mir-150-3p inhibit cancer cell aggressiveness by targeting SPOCK1 in head and neck squamous cell carcinoma. *Auris Nasus Larynx*. **45**, 854–865. https://doi.org/10.1016/j.anl.2017.11.019 (2018).
15. Zhang, Z., Wang, J., Li, J., Wang, X. & Song, W. MicroRNA-150 promotes cell proliferation, migration, and invasion of cervical cancer through targeting PDCD4. *Biomed. Pharmacother.* **97**, 511–517. https://doi.org/10.1016/j.biopha.2017.09.143 (2018).
16. Wang, W. H. et al. MiR-150-5p suppresses colorectal cancer cell migration and invasion through targeting MUC4. *Asian Pac. J. Cancer Prev.* **15**, 6269–6273. https://doi.org/10.7314/apjcp.2014.15.15.6269 (2014).
17. Sun, X., Zhang, C., Cao, Y. & Liu, E. miR-150 suppresses Tumor Growth in Melanoma through downregulation of MYB. *Oncol. Res.* **27**, 317–323. https://doi.org/10.3727/096504018x15228863026239 (2019).
18. Tang, W. et al. MicroRNA-150 suppresses triple-negative breast cancer metastasis through targeting HMGA2. *Onco Targets Ther.* **11**, 2319–2332. https://doi.org/10.2147/ott.S161996 (2018).
19. Li, H. et al. MiR-150 promotes cellular metastasis in non-small cell lung cancer by targeting FOXO4. *Sci. Rep.* **6**, 39001. https://doi.org/10.1038/srep39001 (2016).
20. Lu, W. et al. Long non-coding RNA linc00673 regulated non-small cell lung cancer proliferation, migration, invasion and epithelial mesenchymal transition by sponging miR-150-5p. *Mol. Cancer.* **16**, 118. https://doi.org/10.1186/s12943-017-0685-9 (2017).
21. Cao, M. et al. miR-150 promotes the proliferation and migration of lung cancer cells by targeting SRC kinase signalling inhibitor 1. *Eur. J. Cancer.* **50**, 1013–1024. https://doi.org/10.1016/j.ejca.2013.12.024 (2014).
22. Liu, S. et al. miR-4634 augments the anti-tumor effects of RAD001 and associates well with clinical prognosis of non-small cell lung cancer. *Sci. Rep.* **10**, 13079. https://doi.org/10.1038/s41598-020-70157-0 (2020).
23. Aran, D., Sirota, M. & Butte, A. J. Systematic pan-cancer analysis of tumour purity. *Nat. Commun.* **6**, 8971. https://doi.org/10.1038/ncomms9971 (2015).
24. Aran, D., Hu, Z. & Butte, A. J. xCell: digitally portraying the tissue cellular heterogeneity landscape. *Genome Biol.* **18**, 220. https://doi.org/10.1186/s13059-017-1349-1 (2017).
25. Jiang, P. et al. Signatures of T cell dysfunction and exclusion predict cancer immunotherapy response. *Nat. Med.* **24**, 1550–1558. https://doi.org/10.1038/s41591-018-0136-1 (2018).
26. Maeser, D., Gruener, R. F. & Huang, R. S. oncoPredict: an R package for predicting in vivo or cancer patient drug response and biomarkers from cell line screening data. *Brief. Bioinform.* **22** https://doi.org/10.1093/bib/bbab260 (2021).
27. Wen, Q. et al. FLOT-2 is an independent prognostic marker in oral squamous cell carcinoma. *Int. J. Clin. Exp. Pathol.* **8**, 8236–8243 (2015).
28. Wen, Q. et al. Flot-2 expression correlates with EGFR levels and poor prognosis in surgically resected Non-small Cell Lung Cancer. *PLoS One.* **10**, e0132190. https://doi.org/10.1371/journal.pone.0132190 (2015).
29. Shen, Q., He, Y., Qian, J. & Wang, X. Identifying tumor immunity-associated molecular features in liver hepatocellular carcinoma by multi-omics analysis. *Front. Mol. Biosci.* **9**, 960457. https://doi.org/10.3389/fmolb.2022.960457 (2022).
30. Shi, Y. et al. The structure, expression and function prediction of DAZAP2, a down-regulated gene in multiple myeloma. *Genomics Proteom. Bioinf.* **2**, 47–54. https://doi.org/10.1016/s1672-0229(04)02007-8 (2004).

31. Huang, R. et al. RNA m(6)a demethylase ALKBH5 protects against pancreatic ductal adenocarcinoma via Targeting regulators of Iron Metabolism. *Front. Cell. Dev. Biol.* **9**, 724282. https://doi.org/10.3389/fcell.2021.724282 (2021).
32. Jiang, C., Liu, Y., Wen, S., Xu, C. & Gu, L. In silico development and clinical validation of novel 8 gene signature based on lipid metabolism related genes in colon adenocarcinoma. *Pharmacol. Res.* **169**, 105644. https://doi.org/10.1016/j.phrs.2021.105644 (2021).
33. Hinokuma, H. et al. Distinct functions between ferrous and ferric iron in lung cancer cell growth. *Cancer Sci.* https://doi.org/10.1111/cas.15949 (2023).
34. Mala, U., Baral, T. K. & Somasundaram, K. Integrative analysis of cell adhesion molecules in glioblastoma identified prostaglandin F2 receptor inhibitor (PTGFRN) as an essential gene. *BMC Cancer*. **22**, 642. https://doi.org/10.1186/s12885-022-09682-2 (2022).
35. Krishnan, V. The RUNX Family of Proteins, DNA repair, and Cancer. *Cells* **12** https://doi.org/10.3390/cells12081106 (2023).
36. Shen, Y. et al. Identification of acetyl-CoA carboxylase alpha as a prognostic and targeted candidate for hepatocellular carcinoma. *Clin. Transl Oncol.* **25**, 2499–2513. https://doi.org/10.1007/s12094-023-03137-1 (2023).
37. He, F., Liu, Q., Liu, H., Pei, Q. & Zhu, H. Circular RNA ACACA negatively regulated p53-modulated mevalonate pathway to promote colorectal tumorigenesis via regulating miR-193a/b-3p/HDAC3 axis. *Mol. Carcinog.* **62**, 754–770. https://doi.org/10.1002/mc.23522 (2023).
38. Piotrowski, K. B. et al. ADAM12 expression is upregulated in cancer cells upon radiation and constitutes a prognostic factor in rectal cancer patients following radiotherapy. *Cancer Gene Ther.* https://doi.org/10.1038/s41417-023-00643-w (2023).

Acknowledgements
Not applicable.

Author contributions
HZheng: Conceptualization, Methodology, Software, Data curation. SF: Visualization, Investigation, Funding acquisition. JL: Supervision, Funding acquisition. QW: Supervision, Funding acquisition. HZang: Software, Validation, Writing-Original draft preparation, Writing-Reviewing and Editing, Funding acquisition.

Funding
This work was supported by the National Natural Science Foundations of China (No: 82102805, and 82272722), the Natural Science Foundations of Hunan Province (No: 2023JJ30788), the Fundamental Research Funds for the Central Universities of Central South University (2023ZZTS0843), the Health Commission Scientific Research Program of Hunan Province (No: C202301048453), and the Scientific Research Launch Project for New Employees of the Second Xiangya Hospital of Central South University.

Declarations

Competing interests
The authors declare no competing interests.

Additional information
Supplementary Information The online version contains supplementary material available at https://doi.org/10.1038/s41598-025-85793-7.

Correspondence and requests for materials should be addressed to H.Z.